INVITED PAPER *Special Section on Electronic Displays*

Effect of Impurity in Discharge Gas on High γ Properties of Newly Developed CeSrO Film for Novel Plasma Display Panel

Yasuhiro YAMAUCHI[†a)], **Yusuke FUKUI**[†], **Yosuke HONDA**[†], **Michiko OKAFUJI**[†], **Masahiro SAKAI**[†], **Mikihiko NISHITANI**[†], ***and*** **Yasushi YAMAUCHI**[††], ***Nonmembers***

SUMMARY The discharge properties and chemical surface stability of CeO_2 containing Sr (CeSrO) as the candidate for high-γ protective layer of noble plasma display panels (PDPs) are characterized. CeSrO films have superior chemical stability, because of the decrease in reactiveness on surface due to their fluorite structure. The discharge voltage is 50 V lower than that of MgO films for a pure discharge gas of Ne/Xe = 85/15 at 60 kPa. However the topmost surface, monolayer, of the CeSrO film relevant to the discharge property is hardly recovered from the damage by CO_2 impurity in discharge gas. We can expect that by pumping down to a sufficiently low CO_2 partial pressure (lower than 1×10^{-3} Pa), PDP panels with very high efficiency are realized with CeSrO protective layer.

key words: *PDP, γ, protective layer, discharge, MgO*

1. Introduction

MgO films are widely used as protective layers for plasma display panels (PDPs) due to their high sputtering resistance, superior wall-electron-keeping properties, exo-emission properties and high process resistance. Moreover, the secondary-electron-emission coefficient γ of MgO is high enough for Ne ions, which is necessary for the low voltage plasma discharge [1]. However, the γ of MgO is quite low for Xe ions because the ionization energy of Ne is 22 eV whereas that of Xe is 12 eV [2]. In the Auger-neutralization scheme, only the electrons within the energy range from the vacuum level to the half of the ionization energy of the discharge gas contribute to the secondary-electron-emission, but the valence band top of MgO appears at 8.5 eV from the vacuum level [1]. On the contrary, in order to increase the luminous efficiency, Xe content of the discharge gas of PDPs needs to be raised because UV radiation is emitted by the excited Xe species. Therefore, the development of a high-γ protective layer for Xe ions to replace MgO is strongly required.

Recently, the protective layers with high γ for PDPs have been developed by many research groups. Shinoda et al. [3] and Motoyama et al. [4], [5] have proposed a Sr-CaO protective layer, Kim et al. [6] has researched a MgSr-CaO protective layer and Uchida et al. [7] has reported the characteristics of AC-PDP, where SrO is used as protective layer. We also report on the discharge properties and chemical stability of SrO containing covalent element Zr (SrZrO) [8]. However, the high γ materials based on alkaline-earth oxides, such as CaO, SrO, BaO, SrCaO and SrZrO, have low resistances to the sealing process due to their chemically active characteristics. Impurity, such as carbonate and H_2O, will adsorb to the surface, and will decrease the γ [9]. Therefore, it is quite important to develop the high γ protective layer with high chemical surface stability.

We have developed a CeSrO (CeO_2 containing Sr) protective layer. As the concept, we attempt to prevent carbonation by adding covalent elements. The fourth group elements, such as Ti, Zr, Hf and Ce do not have d electrons because they are tetravalent. In the result, we found that the discharge properties and chemical stability of SrO containing Ce are the best in these four elements. However, the CeSrO does not show high γ property adopted for a large panel such as 42 inch with high uniformity. Thus, we examined the effect of impurity in sealing process and pumping process on high γ properties of CeSrO film with a demountable chamber system. In this paper, we report the discharge characteristics and the chemical stability to the sealing process and the pumping process of CeSrO.

2. Experimental

We prepared test element groups (TEGs) with the CeSrO films which were deposited by an electron beam evaporation method as shown in Table 1. The substrate temperature was 300°C, O_2 gas flow rate was 0.1 sccm, and deposition rate was 0.5 nm/sec. The compact made by sintering a mixture of $SrCO_3$ and CeO_2 powder at 1400°C for two hours in the air was used as the target. We prepared some targets with a different ratio of CeO_2 and $SrCO_3$, and made CeSrO films with different Ce contents. The TEGs had a dielectric layer (ε_r~11) and electrodes to examine discharge parameters. The electrodes were etched into two parts with the gap

Table 1 Typical deposition parameter.

BG pressure	1.2×10^{-6} Pa
Substrate temperature	300 °C
O_2 flow	0.1 sccm
High Voltage	7.5 kV
Beam current	185 mA
Deposition rate	0.5 nm/sec
Thickness	400 nm

Manuscript received February 24, 2012.
Manuscript revised June 6, 2012.

[†]The authors are with Image Devices Development Center, Panasonic Corp., Moriguchi-shi, 570-8501 Japan.
[††]The author is with National Institute of Material Science, Tsukuba-shi, 305-0047 Japan.
a) E-mail: yamauchi.yasuhiro@jp.panasonic.com

DOI: 10.1587/transele.E95.C.1761

by 80 μm (often called main gap). For comparison, we also prepared TEGs with the MgO and SrCaO films in a similar way.

X-ray diffraction (XRD) analysis with CuKα was made in order to identify the constituent phase and crystallinity. The chemical composition and state of the deposited protective layer was identified by using X-ray photoelectron spectroscopy (XPS) obtained by monochromatic AlKα emission. The topmost surface of the protective layer was identified by using meta-stable de-excitation spectroscopy (MDS) [10]–[12] with meta-stable helium (He*). MDS is an extremely surface-sensitive technique because only electrons at the topmost surface contribute to the MDS spectra, which is exactly the same to the plasma discharge of PDPs [13]. Therefore, the MDS has a big advantage in the characterization of the discharge phenomenon, compared with the other techniques.

In order to examine the tolerance to the sealing process, the TEGs were annealed at 500°C for two hours in the air. The discharge characteristic of the each TEG was evaluated by the demountable chamber system: 1) set the TEG in the chamber, 2) evacuate the chamber, 3) anneal the TEG at 480°C for 8 hours in vacuum (under 5×10^{-6} Pa), 4) stop the evacuation after the TEG is cooled down to room temperature, 5) fill the chamber with the discharge gas of Ne/Xe = 85/15, 60 kPa, 6) give aging for two hours, 7) measure the discharge characteristics (Fig. 1). For comparison, we evaluated the discharge characteristics of the each TEG without the annealing in the air. Chemical stability to the sealing process was evaluated by XPS in C1s and the valance band.

Next, we prepared 5, 13 and 42 inch test panels with MgO and $Ce_{0.6}Sr_{0.4}O$ protective layers which were deposited by the electron beam evaporation method. Each panel had a dielectric layer (ε_r~7) and two electrodes with the main gap 40 μm. We gave aging for seven hours and measured the discharge characteristics of the each panel.

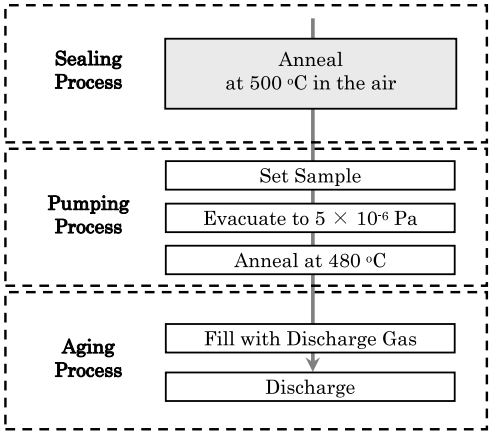

Fig. 1 Process flow of chamber experiment with sealing process.

3. Results and Discussion

3.1 Composition and Crystal Structure

XRD profiles of $Ce_xSr_{1-x}O$ layers are shown in Fig. 2. At the Ce content of $x > 0.5$, several peaks confirming fluorite structure of CeO_2 are observed, and their peaks disappear with decreasing Ce content to be $x = 0.26$. It shows that $Ce_{0.26}Sr_{0.74}O$ consists of amorphous structure. Then, at the Ce content of $x < 0.1$, some peaks confirming rock-salt structure of SrO are observed.

However, their peaks also disappear with decreasing Ce content to be $x = 0.003$, and another peaks confirming $Sr(OH)_2$ are observed. It is assumed to be caused by low chemical stability of $Ce_{0.003}Sr_{0.997}O$. From these results, it was found that the crystal structure of CeSrO changes with increasing Ce content from rock-salt to fluorite with the transition range of amorphous structure.

Moreover, diffraction peaks are shifted by change of a Ce content in CeSrO. Figure 3 shows the lattice constants estimated by the diffraction peaks of (111) plane of CeO_2

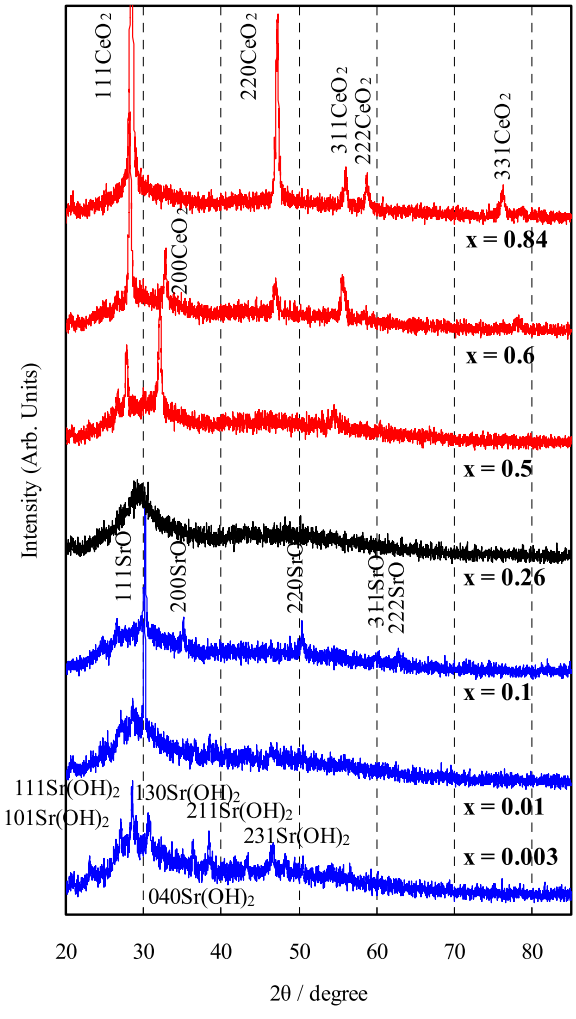

Fig. 2 XRD profiles of $Ce_xSr_{1-x}O$ layers.

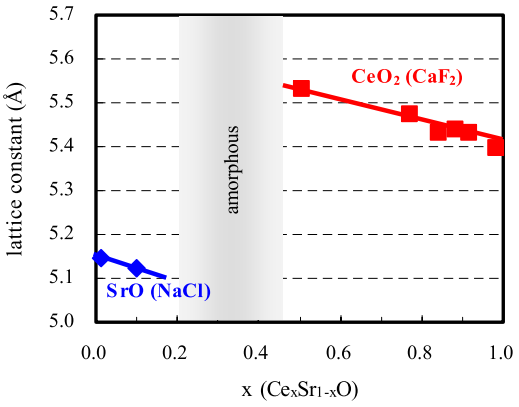

Fig. 3 Relationship between lattice constants and Ce content of CeSrO layers.

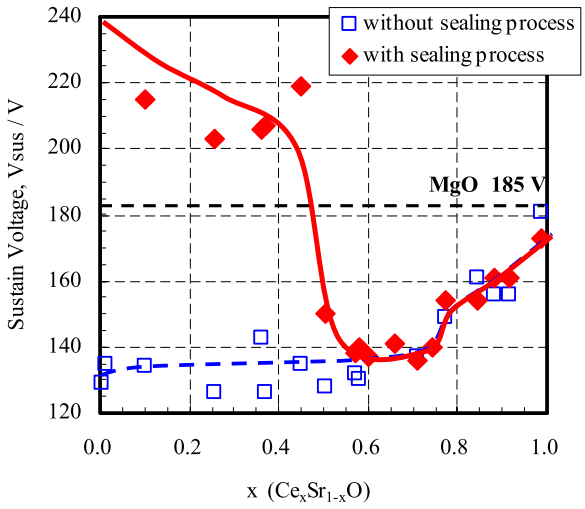

Fig. 4 The sustain voltage of CeSrO as a function of the Ce content of CeSrO layers under the discharge gas of Ne/Xe = 85/15 at 60 kPa.

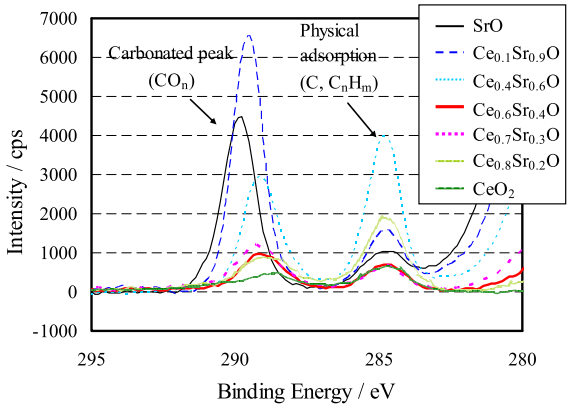

Fig. 5 C1s XPS spectra of $Ce_xSr_{1-x}O$ ($0 \leq x \leq 1$) after annealing at 500°C for two hours in the air.

or (111) plane of SrO with Ce content of CeSrO layers. At the Ce content of $x \geq 0.5$, the lattice constant of fluorite structure decreases from 5.53 Å to 5.39 Å with increasing Ce content to be $x = 1.0$. On the other hand, at the Ce content of $x \leq 0.1$, lattice constant of rock-salt structure decreases from 5.16 Å to 5.12 Å with increasing Ce content to be $x = 0.1$. The ionic radius of Ce^{4+} and Sr^{2+} is 0.97 and 1.18 Å, respectively. Thus, these results suggest that substitution of Ce sites by Sr ions occurs in the fluorite structure, and substitution of Sr sites by Ce ions occurs in the rock-salt structure.

3.2 Discharge Characteristics

The sustain voltage of CeSrO as a function of the ratio of Ce/(Ce+Sr) is shown in Fig. 4. TEGs with deposited CeSrO layer were introduced into the discharge chamber after the annealing process at 500°C in the air as the sealing process. In our experiments, the sustain voltage of MgO as a reference was 185 V. At the Ce content of $x = 1$, i.e. CeO_2, the voltage is 15 V lower than that of MgO, and then, the voltage decreases to be 135 V with decreasing Ce content to be $0.6 \leq x \leq 0.7$. In the Auger neutralization theory, the high density of states at the lower energy band from the vacuum level is needed in order to emit the secondary electron in high-Xe-content discharge gas because the ionization energy of Xe is lower than that of Ne [14]. We consider the γ was increased because the valence band of CeSrO with substitution of Ce sites by Sr ions in the fluorite structure was shifted to lower than that of CeO_2, the high γ was kept even after the annealing process because of the high surface stability. However, the sustain voltage of the TEGs with the sealing process increases to be about 220 V with further decreasing Ce content. This result suggest that the extrinsic gas species are easily adsorbed to the surface of CeSrO consisting of the rock-salt or the amorphous structure, and the γ decreased.

3.3 Chemical State

Figure 5 shows the XPS spectra in C1s of $Ce_xSr_{1-x}O$ ($0 \leq x \leq 1$) layers after the annealing at 500°C for two hours in the air. In these spectra, the peak height around 285 eV which is caused by physical adsorption of hydrocarbon was not deviated so much except $Ce_{0.4}Sr_{0.6}O$. On the other hand, the peak around 290 eV caused by carbonation for $Ce_xSr_{1-x}O$ ($0 \leq x \leq 0.4$) is three times higher than that of $Ce_xSr_{1-x}O$ ($0.5 \leq x \leq 1$). This result shows that $Ce_xSr_{1-x}O$ ($0 \leq x \leq 0.4$) with the rock-salt or the amorphous structure is weak in carbonation, but $Ce_xSr_{1-x}O$ ($0.5 \leq x \leq 1$) has superior chemical stability due to their fluorite structure even after the annealing.

Consequently, it was found that adding adequate amount of Sr in CeO_2 improves discharge characteristics and maintains the chemical surface stability.

Figure 6 shows the XPS spectra in the valence band of $Ce_xSr_{1-x}O$ ($0 \leq x \leq 1$) after the annealing at 500°C for two hours in the air. In $Ce_xSr_{1-x}O$ ($x \leq 0.4$), the peak shift of the valence band top (O2p) to high binding energy caused by carbonation was observed. On the other hand, in $Ce_xSr_{1-x}O$ ($x \geq 0.5$), the valence band top remains at

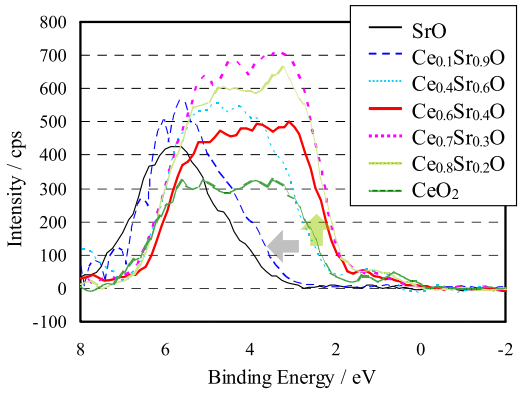

Fig. 6 Valence band XPS spectra of $Ce_xSr_{1-x}O$ ($0 \leq x \leq 1$) after annealing at 500°C for two hours in the air.

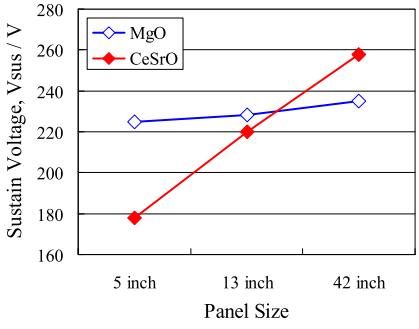

Fig. 7 The sustain voltage of panels with MgO and $Ce_{0.6}Sr_{0.4}O$ protective layers.

low binding energy because of high resistance to carbonation. Moreover, the density of states of valence band top for $Ce_xSr_{1-x}O$ ($0.6 \leq x \leq 0.8$) was higher than that of CeO_2 which is probably related to the substitution of Ce sites by Sr ions.

3.4 Panel Property

Figure 7 shows the sustain voltage of the panels with MgO and $Ce_{0.6}Sr_{0.4}O$ protective layers. In the 5 inch panel, the sustain voltage of $Ce_{0.6}Sr_{0.4}O$ was 47 V lower than that of MgO and the value is similar to that of the chamber experiment. However, when the panel size was larger, the voltage with $Ce_{0.6}Sr_{0.4}O$ protective layer rose and that of $Ce_{0.6}Sr_{0.4}O$ was 23 V higher than that of MgO in the 42 inch panel.

3.5 Further Analysis on Carbonation

The $Ce_xSr_{1-x}O$ ($0.6 \leq x \leq 0.7$) protective layer has superior chemical stability against annealing at 500°C in the air, and the sustain voltage is 50 V lower than that of MgO in the chamber experiment. However, the CeSrO does not show high γ property adopted for the larger panel such as 42 inch with high uniformity. Thus, we examined the effect of impurity in the sealing process and the pumping process on the high γ properties of CeSrO film, whose Ce content is 0.6, with a different demountable chamber system.

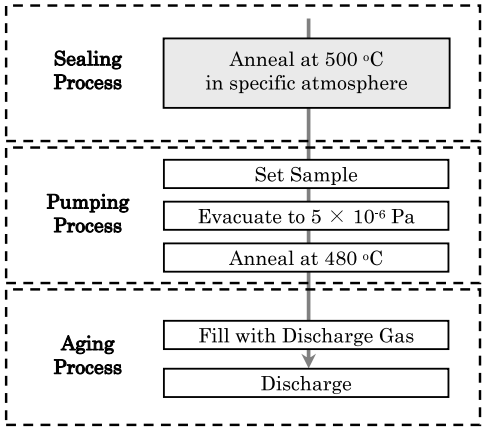

Fig. 8 Process flow of chamber experiment for effect of CO_2 remaining in sealing process.

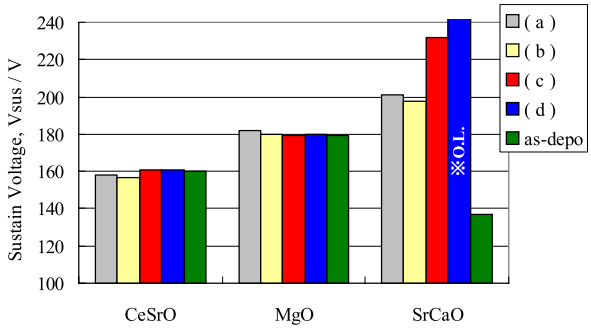

Fig. 9 The sustain voltages of CeSrO, MgO and SrCaO by annealing in (a) dry-air, (b) air including 10% CO_2, (c) air bubbled in 55°C water or (d) air including 10% CO_2 bubbled in 55°C water. The voltages of CeSrO and MgO do not change by annealing in air including CO_2 and H_2O. The voltage of SrCaO rises by over 64 V by annealing in dry-air or air including CO_2 and H_2O. The voltage of SrCaO could not be measured when annealed in the air including CO_2 and H_2O.

3.5.1 Sealing Process Analysis

First, we supposed the CeSrO protective layer was deteriorated in the sealing process, and experimented as follows. We prepared TEGs with the CeSrO, whose Ce content is 0.6, MgO and SrCaO protective layers which were deposited by the electron beam evaporation method. The TEGs had a dielectric layer ($\varepsilon_r \sim 11$) and electrodes (main gap 80 μm). As the sealing process, the each TEG was annealed at 480°C for 30 minutes in (a) dry-air, (b) air including 10% CO_2, (c) air bubbled in 55°C water or (d) air including 10% CO_2 bubbled in 55°C water. The discharge characteristics of the each TEG were evaluated by the chamber experiment (Fig. 8).

Figure 9 shows the sustain voltages of the each TEG annealed in (a)–(d). In CeSrO, even if there were CO_2 and H_2O in the sealing process, the protective layer was not deteriorated and the sustain voltage did not change. It is similar for MgO (the voltages were slightly different to that of Fig. 4, because a different chamber system was utilized). On the other hand, in SrCaO, the sustain voltage rose by 64 V

by the annealing in dry-air (a). The voltage rose by 95 V by the annealing in air bubbled in 55°C water (c). In addition, when the SrCaO TEG was annealed in the air including CO_2 bubbled in 55°C water (d), the voltage could not be measured (over 300 V).

3.5.2 Pumping Process Analysis

Secondly, we supposed the CeSrO protective layer is deteriorated by impurity remaining in pumping process [15], [16], and experimented as follows: 1) set CeSrO, whose Ce content is 0.6, MgO and SrCaO TEGs without sealing process, 2) evacuate the chamber, 3) flow CO_2 gas and control the pressure 1×10^{-5}~1×10^{-1} Pa, 4) anneal the TEGs at 480°C for 8 hours, 5) stop the evacuate and CO_2 flow after the TEGs are cooled down to room temperature, 6) fill the chamber with the discharge gas of Ne/Xe = 85/15, 60 kPa, 7) give aging for two hours, 8) measure the discharge characteristics (Fig. 10). MgO and SrCaO protective layers were also examined.

The sustain voltages of CeSrO, MgO and SrCaO are shown as a function of the pressure of CO_2 gas remaining in the pumping process in Fig. 11. With increasing the CO_2 gas pressure over 1×10^{-3} Pa, the sustain voltage of the each protective layer was increased. In CeSrO, when the pressure of CO_2 gas was over 1×10^{-3} Pa, the sustain voltage rose; the voltage at 1×10^{-2} Pa was 35 V higher than that at 1×10^{-5} Pa. In MgO, the voltage at 1×10^{-2} Pa was 20 V higher than that at 1×10^{-5} Pa. In SrCaO, the voltage at 1×10^{-2} Pa was 29 V higher than that at 1×10^{-5} Pa.

3.5.3 Recovering Effect of Anneal in Vacuum

From these results, it was found that the CeSrO is not influenced by CO_2 and H_2O in the sealing process, but the pumping process should be performed in the lower CO_2 residue than 1×10^{-3} Pa to keep the high γ property.

This seems to show that CeSrO films are deteriorated by CO_2 remaining in the pumping process, but that the deteriorated films are hardly recovered by the annealing in the pumping process and the aging when CO_2 is remained.

To examine the possibility of the recovery, we carried out the surface characterization of the CeSrO film, whose Ce content is 0.6, through the pumping process (Fig. 10) with XPS and MDS. The pressure of CO_2 gas remaining in the pumping process was from 1×10^{-5} to 1×10^{-2} Pa.

Figure 12 shows valence band spectra by XPS and MDS. The sustain voltage at the pressure of CO_2 1×10^{-2} Pa

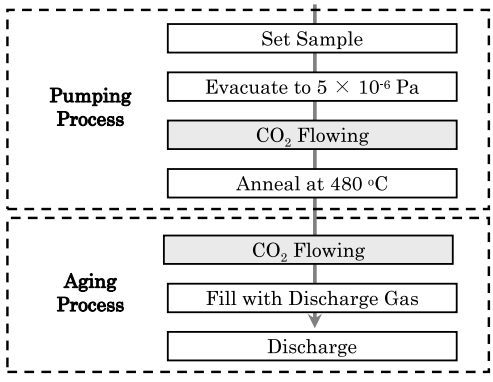

Fig. 10 Process flow of the chamber experiment to examine the effect of CO_2 remaining in the pumping process.

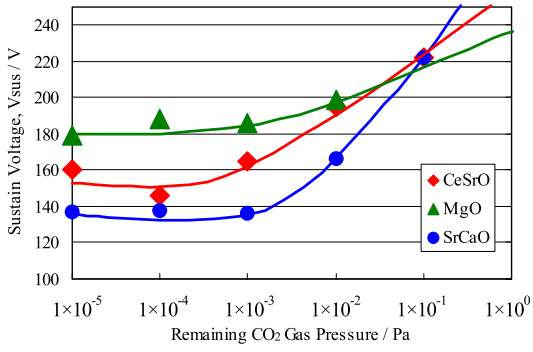

Fig. 11 The sustain voltages of CeSrO, MgO and SrCaO as a function of the pressure of CO_2 gas remaining in pumping process. The sustain voltage of the each protective layer was increased with increasing the CO_2 gas pressure.

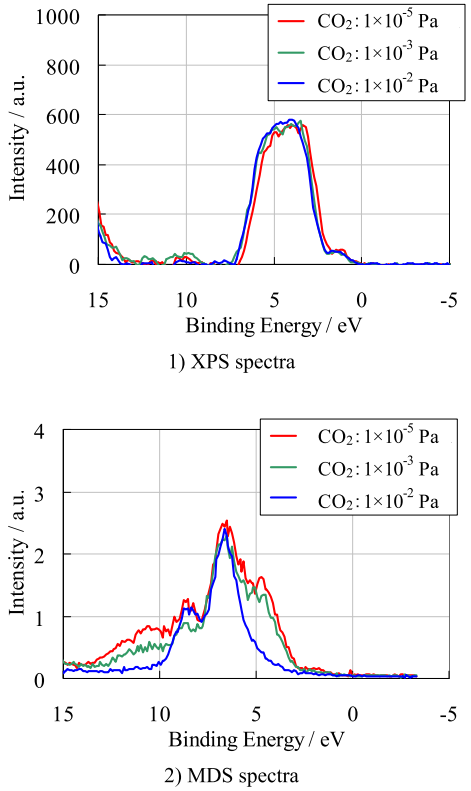

Fig. 12 XPS and MDS spectra of CeSrO film for different CO_2 pressures in the chamber experiment (Fig. 11). The pressure of CO_2 gas remaining in pumping process is from 1×10^{-5} to 1×10^{-2} Pa. XPS spectra do not show appreciable difference. On the other hand, MDS spectra show that when the remaining CO_2 gas pressure was high, the density of states near the valence band top was low.

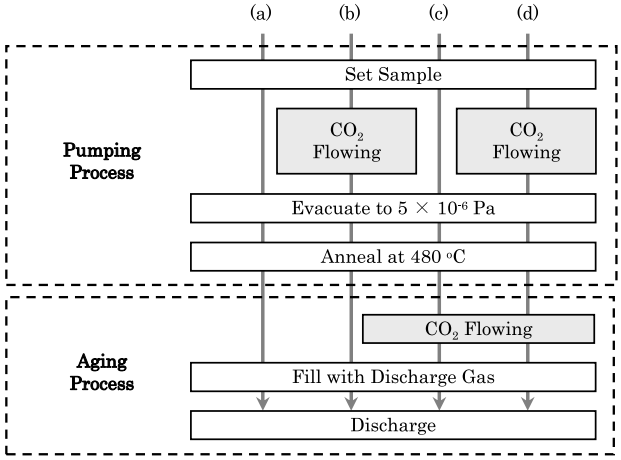

Fig. 13 Process flow of the chamber experiment to examine the effect of CO_2 in discharge gas. (a) CO_2 is not introduced. CO_2 introduced (b) only in anneal process, (c) only in discharge gas, (d) both in anneal process and discharge gas.

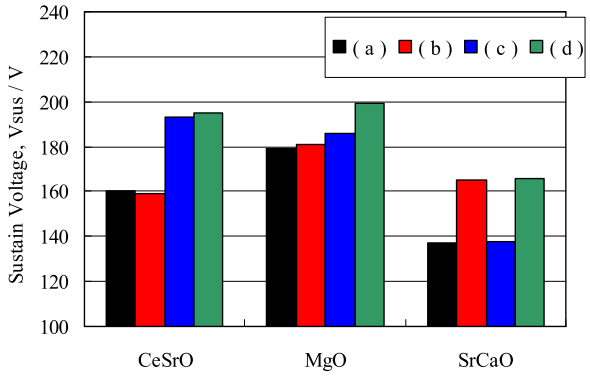

Fig. 14 The sustain voltages of CeSrO, MgO, and SrCaO after sealing process and after aging for two hours. (a) CO_2 is not introduced. CO_2 introduced (b) only in anneal process, (c) only in discharge gas, (d) both in anneal process and discharge gas. The each remaining CO_2 gas pressure was 1×10^{-2} Pa.

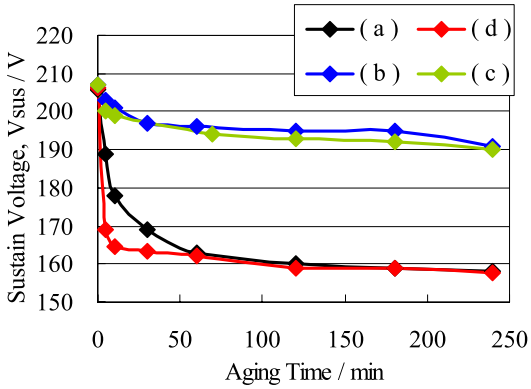

Fig. 15 The sustain voltages of CeSrO as a function of the aging time for various conditions of the sealing process. (a) CO_2 is not introduced. CO_2 introduced (b) only in anneal process, (c) only in discharge gas, (d) both in anneal process and discharge gas. The each remaining CO_2 gas pressure was 1×10^{-2} Pa.

was 35 V higher than that at 1×10^{-5} Pa, but the XPS spectra showed almost no difference. On the other hand, MDS spectra showed that when the remaining CO_2 gas pressure was high, the density of states near the valence band top was low. The characterization region of MDS corresponds to the topmost surface while the region of XPS corresponds to several nm inside from the topmost surface of the material.

Thus, the topmost surface, or monolayer, of the film governs the discharge property and is hardly recovered from the damage due to the residual CO_2 impurity of the atmosphere in the pumping process.

3.5.4 Effect of CO_2 in Pumping and in Aging

To examine the effect of impurity in the discharge gas, we examined the discharge characteristics of CeSrO, whose Ce content is 0.6, MgO and SrCaO TEGs after the sealing process (a) without CO_2, or with CO_2. Where CO_2 were included (b) only in the anneal process, (c) only in the discharge gas or (d) both in the anneal process and in the discharge gas. The CO_2 gas pressure was set to be 1×10^{-2} Pa for the each case and the each TEG was aged for two hours (Fig. 13).

The sustain voltages of CeSrO, MgO, and SrCaO through the each process and after aging for two hours are shown in Fig. 14. The sustain voltages of CeSrO after the each process as a function of the aging time are shown in Fig. 15.

In CeSrO, the voltage did not rise when CO_2 remained only in anneal process (b), but the voltage rose by 33 V when CO_2 remained in discharge gas (c and d). Similarly, in MgO, the voltage rose by 7~20 V when CO_2 remained in the discharge gas (c and d). On the other hand, the different result was obtained in SrCaO. In SrCaO, the voltage did not change when CO_2 remained only in the discharge gas (c), but the voltage rose by 28 V when CO_2 remained in the anneal process (b and d). Considering this result and the data shown in Fig. 9, The topmost surface of the CeSrO film may be deteriorated in the sealing process, but it is recovered in the pumping process when performed under the low CO_2 residue. However, as indicated in Fig. 14, The topmost surface of the SrCaO film is deteriorated by CO_2 in the sealing process, and the deteriorated film is never recovered by the pumping process and the aging.

Consequently, we consider that the remaining CO_2 in the pumping process for a larger panel such as 42 inch is not low enough to show high γ property uniformly even for the CeSrO film.

4. Conclusions

We have characterized the discharge characteristics and chemical surface stability of CeO_2 containing Sr (CeSrO), and came to the conclusions stated below.

(1) Adding adequate amount of Sr in CeO_2 improves the discharge characteristics such as sustain voltage, which is 50 V lower than that of MgO under a pure discharge gas of Ne/Xe

= 85/15 at 60 kPa.
(2) CeSrO films consisting of fluorite structure have superior chemical stability.
(3) Especially, $Ce_{0.6}Sr_{0.4}O$ film has superior discharge properties and high γ properties, and we have confirmed that the film has high density of states near valence band top by MDS, which shows that the topmost surface, monolayer, of the protective layer governs the discharge property. When the remaining CO_2 gas pressure is lower than 1×10^{-3} Pa, the $Ce_{0.6}Sr_{0.4}O$ film is recovered from the carbonation by pumping process and aging, and shows high γ property.
(4) SrCaO film is easily deteriorated by CO_2 in anneal process, and the deteriorated film is never recovered in pumping process and in aging.

From these results, we can expect that when pumping process is performed in a low CO_2 residue atmosphere (lower than 1×10^{-3} Pa), PDP panels with very high efficiency are realized with CeSrO protective layer.

References

[1] G. Oversluizen, T. Dekker, M.F. Gillies, and S.T. de Zwart, "High-Xe-content high-efficacy PDPs," J. SID, vol.12, no.1, pp.51–55, March 2004.
[2] L.A. Levin, S.E. Moody, E.L. Klosterman, R.E. Center, and J.J. Ewing, "Kinetic model for long-pulse XeCl laser performance," IEEE J. Quantum Electron., vol.QE-17, no.12, pp.2282–2289, Dec. 1981.
[3] T. Shinoda, H. Uchiike, and S. Andoh, "Low-voltage operated AC plasma-display panels," IEEE Trans. Electron Devices, vol.26, no.8, pp.1163–1167, Aug. 1979.
[4] Y. Motoyama, Y. Murakami, M. Seki, T. Kurauchi, and N Kikuchi, "SrCaO protective layer for high-efficiency PDPs," IEEE Trans. Electron Devices, vol.54, no.6, pp.1308–1314, June 2007.
[5] Y. Motoyama and T. Kurauchi, "Protective layer for high-efficiency PDPs driven at low voltage," J. SID, vol.14, no.5, pp.487–492, May 2006.
[6] R. Kim, Y. Kim, J. Cho, and J.W. Park, "Luminous efficiency and secondary electron emission characteristics of alternating current plasma display panels with MgO-SrO-CaO protective layers," J. Vac. Sci. Technol. A, vol.18, no.5, pp.2493–2496, Sept./Oct. 2000.
[7] G. Uchida, K. Uchida, H. Kajiyama, and T. Shinoda, "Analysis of optical emission spectra from AC-PDP operated at lower voltage," Proc. SID, vol.3, no.39, pp.1762–1765, 2008.
[8] Y. Fukui, Y. Honda, Y. Yamauchi, M. Okafuji, M. Sakai, M. Nishitani, and Y. Takata, "Discharge properties and chemical stability of SrZrO films," J. SID, vol.18, no.12, pp.1090–1094, 2010.
[9] M. Sakai, S. Hatta, Y. Fukui, Y. Honda, M. Okafuji, Y. Yamauchi, M. Nishitani, and Y. Takata, "Analysis of the deterioration of secondary electron emission coefficient of protective layers formed by alkaline-earth oxides for plasma display panels," Proc. IDW, vol.13, no.15, pp.1881–1884, 2008.
[10] M. Nishitani, Y. Morita, M. Terauchi, Y. Yamauchi, K. Yoshino, M. Sakai, Y. Takata, and Y. Yamauchi, "Surface characterization of MgO:Al N films with meta-stable de-excitation spectroscopy and x-ray photoelectron spectroscopy," J. SID, vol.19, no.1, pp.8–14, 2011.
[11] X. Sun, S. Förster, Q. Li, M. Kurahashi, T. Suzuki, J. Zhang, Y. Yamauchi, G. Baum, and H. Steidl, "Spin-polarization study of CO molecules adsorbed on Fe(110) using metastable-atom deexcitation spectroscopy and first-principles calculations," Phys. Rev. B, vol.75, no.3, 035419, 2007.
[12] X. Sun, Y. Yamauchi, M. Kurahashi, T. Suzuki, Z.P. Wang, and S. Entani, "Spin polarization study of benzene molecule adsorbed on Fe(100) surface with metastable-atom deexcitation spectroscopy and density functional calculations," J. Phys. Chem. C, vol.111, no.42, pp.15289–15298, 2007.
[13] M. Kurahashi and Y. Yamauchi, "A metastable de-excitation spectroscopy (MDS) study on oxygen adsorption on a polycrystalline zirconium surface," Surface Sci., vol.420, pp.259–268, 1999.
[14] Y. Motoyama, and F. Sato, "Calculation of secondary electron emission yield γ from MgO surface," IEEE, Trans. Plasma Science, vol.34, no.2, pp.336–342, April 2006.
[15] S.J. Kwon and C.-K. Jang, "Effects of base vacuum level on discharge characteristics in vacuum in-line sealing process for high efficient PDP," J. Inf. Disp, vol.5, pp.7–11, 2004.
[16] T. Kweon, E. Jung, C. Park, J. Heo, H. Park, J. Kim, H. Tae, and E. Heo, "Efficiency improvement characteristics under exhaust method and Xe gas contents in AC PDP," Proc. IDW, vol.2, no.16, pp.939–942, 2009.

Yasuhiro Yamauchi received his B.E and M.E. degrees in engineering science from Osaka University, Japan, in 2005 and 2007, respectively. In 2007, he joined Panasonic Corporation, where he is now working at the Image Device Development Center of the Corporate R&D Division.

Yusuke Fukui received his M.E. degree in material engineering from the Tokyo Institute of Technology, Japan, in 2004. In 2004, he joined Panasonic Corp., where he is now working at the Image Device Development Center of the Corporate R&D Division. He received his Ph.D. in material engineering from the Tokyo Institute of Technology in 2008.

Yosuke Honda received his B.E. and M.E. degrees in applied chemistry from Tohoku University, Japan, in 2003 and 2005, respectively. In 2005, he joined Panasonic Corp, where he is now working at the Image Device Development Center of the Corporate R&D Division.

Michiko Okafuji is now working at the Image Devices Development Center, Panasonic Corp.

Masahiro Sakai received his B.E. and M.E. degrees in industrial chemistry from the University of Tokyo, Japan, in 1990 and 1992, respectively. He is now working at the Image Device Development Center of Panasonic Corp. Since 2008, he has been an associate editor of the IEEE Journal of Display Technology.

Mikihiko Nishitani received his B.E. and M.E. degrees in applied physics from Osaka University, Japan, in 1978 and 1980, respectively. In 1980, he joined Matsushita Electric Industrial Co., Ltd. Since 1980, he has been at the Central Research Laboratories. He received his D.Eng. degree in applied physics on compound semiconductor material science and processes from Osaka University in 1998. Since 2002, he has been at the Image Devices Development Center, Matsushita (presently Panasonic), Osaka, researching and developing plasma-display.

Yasushi Yamauchi studied experimental physics at the Department of Applied Physics, Osaka University, and then in 1985 he received his doctoral degree in surface science. In the same year, he joined the National Institute for Material Science and has worked there ever since. Presently, his specific interests are centered in exploring spin-sensitive surface phenomena and beam technologies associated with future device development.